IJBEM
Vol. 7, No. 1, 2005

An In-Principle Method for Measuring Cardiac Tissue Fibre Rotation

B. M. Johnston and P. R. Johnston
School of Science, Griffith University, Queensland, Australia

Abstract— **Four electrode techniques have long been used to determine conductivity parameters in cardiac tissue. This paper introduces a mathematical model and solution technique to theoretically analyse electrode configurations, specifically allowing for plunge electrodes. In particular, the focus is on using four electrode configurations to determine fibre rotation in cardiac tissue. Two configurations are analysed, the first with the four electrodes collinear and the second consisting of two probes a fixed distance apart, with the current electrodes on one probe and the measuring electrodes on the other. It is found that the second electrode configuration can yield a value for the fibre rotation under the assumptions of the model.**

Keywords— **Bidomain model, electrodes, electromagnetic field simulation, fibre rotation**

I. Introduction

It has been shown previously that cardiac tissue anisotropy plays a vital role in several aspects of electrocardiography; for example, in modelling ST segment shift in subendocardial ischaemia [1], [2], [3] and in studies of defibrillation efficacy [4]. One part of this anisotropy comes from the differing electrical conductivity in the intra- and extracellular spaces, both longitudinally and transversely. Another part of this anisotropy comes from the fact that the sheets of fibres rotate relative to one another as they move from the epicardium to the endocardium.

Much work has been carried out to try to determine the above conductivity values [5], [6], [7]. Generally, these methods are based on the cable model of electric propagation through the tissue and the conductivity values are determined either from measurement of the amplitudes of the intracellular and extracellular action potentials, or by independently measuring the longitudinal and transverse action potential propagation velocities [8].

Another approach has been the use of a multi-electrode model to determine the conductivity values. The original idea of Plonsey and Barr [9] is to use a four electrode device placed on the epicardium, firstly along the fibres and secondly at right angles to them. An extension of this idea by Le Guyader *et al.* [10] involves using a probe consisting of two orthogonal rows of four electrodes [11]. The spacing of the electrodes is of the order of the length constant of the fibres. This probe is also placed on the epicardium and AC currents of varying frequency are injected. The conductivity parameters are calculated using a minimisation procedure which also yields other electrical properties of the tissue, such as junction capacitance and junction conductivity. Recently, Barr and Plonsey [12] have proposed using a single vertical probe, containing a combination of optical transmembrane potential sensors and extracellular electrodes, to find cardiac conductivities. However, none of these methods can determine the fibre rotation within the cardiac tissue.

Generally, fibre rotation has been determined from detailed morphological studies [13] or by actually slicing away the fibres layer by layer [14]. Such studies are difficult and time-consuming.

The recent advent of silver wire plunge electrodes [15], which can be placed in the cardiac tissue without causing significant injury currents, has provided the opportunity to employ new electrodes and new methodologies to determine the rotation of cardiac fibres. Here, two four electrode techniques are proposed and analysed theoretically as potential methods for finding the degree of fibre rotation. The first consists of one probe, containing four electrodes, which is injected into the cardiac tissue. The second involves placing two probes into the tissue, the first probe providing fixed current sources and the second measuring the resulting potential.

In the next section, a mathematical model, which takes account of many features of the cardiac tissue, is proposed and a solution method is discussed. The following section presents results of the numerical simulation as well as a methodology for using these electrodes to determine the fibre rotation. There is also a discussion of the potential of these methods. Finally, there is a discussion of the limitations of the mathematical model and some future directions.

II. Methods

A. Governing Equations

Since the idea of the proposed method is to measure the local fibre rotation, it is assumed that the cardiac tissue can be represented by a block of tissue, finite in the x and y directions with a length of $2L$ in each direction. It is also assumed that the epicardium is represented by the plane at $z = 0$ and the endocardium is represented by the plane at $z = 1$, which is in contact with a volume of blood extending to ∞ in the positive z direction.

A bidomain model [16], [17], [18] is used to account for the intracellular and extracellular regions of the tissue. The bidomain equations for the intracellular and extracellular potentials, ϕ_i and ϕ_e, respectively are

$$\nabla \cdot (\mathbf{M}_i \nabla \phi_i) = \beta / R_m (\phi_i - \phi_e) \tag{1}$$

$$\nabla \cdot (\mathbf{M}_e \nabla \phi_e) = -\beta / R_m (\phi_i - \phi_e) - I_s \tag{2}$$

where β is the surface to volume ratio of the cells, R_m is the specific membrane resistance, I_s is an external current source per unit volume and $\mathbf{M}_e$, $\mathbf{M}_i$ are conductivity tensors which reflect anisotropy in the cardiac tissue.

Finally, in the blood, which is a source-free region, the electric potential, ϕ_b, is governed by Laplace's equation

$$\nabla^2 \phi_b = 0. \tag{3}$$

B. Conductivity Tensor

The electrical anisotropy of cardiac tissue comes from the fibrous nature of the tissue, with electrical conductivity being greater along the fibres than across them. Hence, four conductivity values are required: $\sigma_l^i, \sigma_t^i, \sigma_l^e, \sigma_t^e$, where the superscripts i and e refer to the intra- and extracellular domains respectively, and the subscripts l and t refer to the longitudinal and transverse directions respectively.

It will be assumed that the rotation of the fibres varies linearly with depth [19] and that the fibre layers are parallel to the epicardium [14]. These assumptions imply that the conductivity tensors can be written as

$$\mathbf{M}_k(x,y,z) = \begin{pmatrix} (\sigma_l^k - \sigma_t^k)c^2 + \sigma_t^k & (\sigma_l^k - \sigma_t^k)cs & 0 \\ (\sigma_l^k - \sigma_t^k)cs & (\sigma_l^k - \sigma_t^k)s^2 + \sigma_t^k & 0 \\ 0 & 0 & \sigma_t^k \end{pmatrix} \tag{4}$$

where $k = i$ or e, $c = \cos\psi(z)$ and $s = \sin\psi(z)$ and $\psi(z) = \alpha z$, where α is the total fibre rotation angle through the tissue which lies between 0 and 180° [13]. The model assumes that the fibres on the epicardium are aligned with the positive x-axis and the fibre sheets rotate anticlockwise from the epicardium to the endocardium.

C. Boundary Conditions

To solve the differential equations (1), (2) and (3) a set of boundary conditions is required. Assuming that the epicardium is insulated means that

$$\text{at z} = 0; \frac{\partial \phi_\text{e}}{\partial \text{z}} = \frac{\partial \phi_\text{i}}{\partial \text{z}} = 0. \tag{5}$$

Further, at the interface between the tissue and the blood, there is continuity of extracellular potential and current, but the intracellular space is insulated by the extracellular space [20]; that is,

$$\text{at z} = 1; \phi_\text{e} = \phi_\text{b}, \sigma_\text{b}\frac{\partial \phi_\text{b}}{\partial \text{z}} = \sigma_\text{t}^\text{e}\frac{\partial \phi_\text{e}}{\partial \text{z}}, \frac{\partial \phi_\text{i}}{\partial \text{z}} = 0. \tag{6}$$

Since the blood mass is assumed infinite in the positive z-direction, $\phi_b \to 0$ as $z \to \infty$. Finally, the x and y boundaries of the domain are insulated so the derivatives of ϕ_e and ϕ_i in the x and y directions at these boundaries are zero.

D. Solution Method

Assume ϕ_e and ϕ_i are given by

$$\begin{aligned} \phi_k(x,y,z) = \sum_{n=0}^{\infty}\sum_{m=0}^{\infty} & C_{nm}^k(z)\cos m\pi y \cos n\pi x \\ & + D_{nm}^k(z)\sin m\pi y \cos n\pi x \\ & + E_{nm}^k(z)\cos m\pi y \sin n\pi x \\ & + F_{nm}^k(z)\sin m\pi y \sin n\pi x \end{aligned} \tag{7}$$

for k=i or e and substitute these into the differential equations. This gives a coupled system of ordinary differential equations in z for the coefficients $C_{nm}^k(z)$, $D_{nm}^k(z)$, $E_{nm}^k(z)$ and $F_{nm}^k(z)$. These ordinary differential equations need to be solved numerically and this is achieved using a simple one dimensional finite difference method. Application of the finite difference method yields a banded system of linear algebraic equations which are solved using standard techniques [21] to give the required coefficients. Once the coefficients are found, the potentials can be obtained by summation of the above series.

The advantage of this approach over a full numerical approach or a Fourier Transform approach [1], [2], [10] is that the potentials are calculated only at points at which they are required. In particular, it is only necessary to calculate the potentials at the measuring electrodes.

E. Electrode Configurations

The idea of this paper is to theoretically analyse electrode placements to determine fibre rotation in cardiac tissue.

As a simple first example, consider the single probe containing four electrodes, shown in Fig. 1. The probe is inserted into the cardiac tissue normal to the epicardium, and consists of two current source electrodes and two electrodes measuring the potential difference. The probe is the direct analogue of that proposed by Plonsey and Barr [9], except that here it is inserted into the cardiac tissue instead of lying along the surface. For the purpose of the simulations presented here, the distance between the current injection electrodes is set at 600 μm with the potential measurement electrodes 200 μm apart, placed evenly between the current electrodes. The top current injection electrode was placed 3mm and later 7mm below the epicardium.

As a second example, consider a new four electrode configuration. The configuration consists, firstly, of two current sources placed on a probe and inserted a fixed distance into the cardiac tissue (Fig. 2). A second probe is used to record the electric potential generated by the current source. The measuring electrodes on this probe correspond exactly to those in Fig. 1, except that the second probe is moved a fixed distance away in the x direction. This electrode configuration differs from previous four electrode configurations [9], [10] in that the four electrodes are no longer collinear. For the simulations performed, the two probes are placed a distance

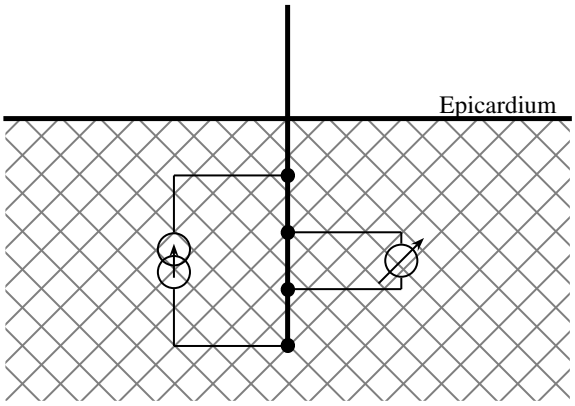

Fig. 1. Schematic diagram for the single probe configuration. Diagram is not to scale.

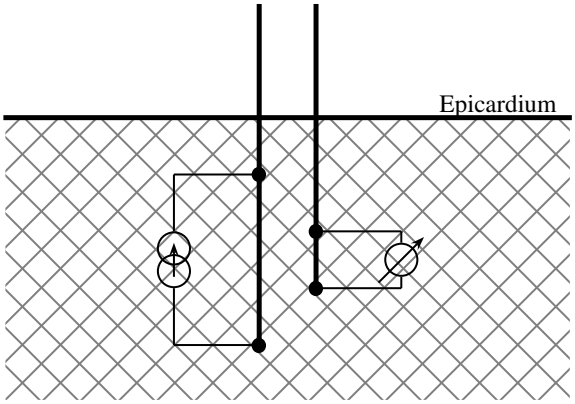

Fig. 2. Schematic diagram for the two probe configuration. Diagram is not to scale.

of 200 μm apart and the top current electrode is placed at a series of distances below the epicardium.

The two electrode configurations proposed above will be used to study the effects of fibre rotation on the potential difference between the two measuring electrodes.

F. Modelling Parameters

The method outlined here is based on the assumption that the longitudinal and transverse electrical conductivity values in both the intra- and extracellular spaces are known already. For the purpose of the simulations presented here, these conductivity values are taken to be $\sigma_l^i = \sigma_l^e = 0.0026$ S/cm, $\sigma_t^i = 0.00026$ S/cm and $\sigma_t^e = 0.00104$ S/cm. This provides a nominal set of conductivities, found using Roth's [22] recipe, based on σ_l^i calculated as the mean value of data from Clerc [5], Roberts *et al.* [6] and Roberts and Sher [7]. The conductivity of blood, σ_b, is taken to be 0.0067 S/cm. The block of tissue modelled was 1 cm thick and 2 cm in each of the x and y directions (that is, L=1). The values of R_m=9100 Ω cm^2 and β=2000 cm^{-1} are from Weidmann [23] and Plonsey and Barr [9] respectively. A 5 μA current I_s is applied.

III. Results and Discussion

Firstly, the potential difference is calculated at the measuring electrodes on the single probe described above. It was found that, for each fibre rotation considered, there was no difference in the potentials recorded. Hence, this type of electrode would be of no use in determining the fibre rotation through the cardiac tissue. This is perhaps not surprising as any needle inserted in the fashion described above would form an axis of rotation for the fibres.

Fig. 3 shows plots of the potential difference on the measurement electrodes for the two probe configuration, plotted as a function of fibre rotation. The maximum fibre rotation considered was 180°, as this was believed to be the highest degree of fibre rotation observed [13]. Each line in the plot corresponds to a different depth of the top current electrode. The plot shows two distinct types of lines. When the electrodes are inserted to a point in the upper half of the tissue ($z < 0.5$), the curve is a monotonically decreasing function of the degree of fibre rotation. However, when the electrodes are inserted to a point in the lower half of the tissue ($z > 0.5$), then the curve reaches a minimum and then starts to increase again. From this figure it can be observed that if the electrodes were inserted to a point in the upper half plane and a potential difference recorded, then a unique value for the fibre rotation throughout the whole tissue could be obtained using the appropriate curve in the figure.

IV. Conclusions

This paper has presented an in-principle method for determining cardiac tissue fibre rotation, based on a mathematical model of the cardiac tissue and a four electrode measuring

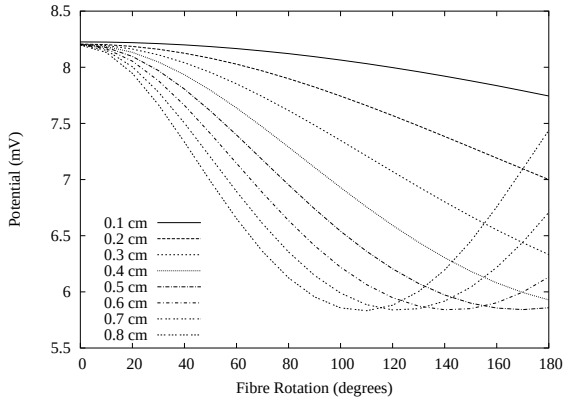

Fig. 3. Potential differences measured using the two probe approach for varying degrees of fibre rotation and depth of the top current injection electrode.

system using two vertical probes. The idea is to use the model to determine a plot of potential difference versus fibre rotation at a given depth of the top current electrode, then measure the potential difference using the electrode configuration described and read off the fibre rotation from the plot.

The proposed method does have some limitations; the principal one is that the method can only be applied in the region of the ventricular wall where the fibre sheets are almost parallel to the epicardium [14]. However, near the base and the apex of the heart, this assumption is no longer valid. Secondly, it may not be the case that the fibre rotation varies linearly with depth; however, this is a reasonably common assumption used in modelling [19]. To overcome this problem, it may be necessary to make recordings at more than one depth.

This two probe configuration is not the only one that allows fibre rotation to be determined. For example, the 'widely-spaced' electrode set of Barr and Plonsey [12], adjusted so that the current and measuring electrodes are on separate probes, is suitable, as is the two probe configuration discussed above but with a wider probe separation, say 1 mm. However, it was found that the closer probe separation produced potential differences in the millivolt range as compared with the tenth of millivolt range at wider separations.

ACKNOWLEDGMENT

This work was funded by the Australian Research Council.

REFERENCES

[1] Peter R. Johnston, David Kilpatrick, and Chuan Yong Li, "The importance of anisotropy in modelling ST segment shift in subendocardial ischaemia," *IEEE Transactions on Biomedical Engineering*, vol. 48, no. 12, pp. 1366–1376, December 2001.

[2] Peter R. Johnston and David Kilpatrick, "The effect of conductivity values on ST segment shift in subendocardial ischaemia," *IEEE Transaction on Biomedical Engineering*, vol. 50, no. 2, pp. 150–158, February 2003.

[3] Peter R. Johnston, "A cylindrical model for studying subendocardial ischaemia in the left ventricle," *Mathematical Biosciences*, vol. 186, no. 1, pp. 43–61, 2003.

[4] Y. Wang, D. R. Haynor, and Y. Kim, "An investigation of the importance of myocardial anisotropy in finite–element modelling of the heart: methodology and application to the estimation of defibrillation efficacy," *IEEE Transactions on Biomedical Engineering*, vol. 48, no. 12, pp. 1377–1389, December 2001.

[5] L. Clerc, "Directional differences of impulse spread in trabecular muscle from mammalian heart," *Journal of Physiology*, vol. 255, pp. 335–346, 1976.

[6] D. E. Roberts, L. T. Hersh, and A. M. Scher, "Influence of cardiac fiber orientation on wavefront voltage, conduction velocity and tissue resistivity in the dog," *Circ. Res.*, vol. 44, pp. 701–712, 1979.

[7] D. E. Roberts and A. M. Scher, "Effects of tissue anisotropy on extracellular potential fields in canine myocardium in situ," *Circ. Res.*, vol. 50, pp. 342–351, 1982.

[8] R. M. Gulrajani, *Bioelectricity and Biomagnetism*, John Wiley and Sons, 1998.

[9] R. Plonsey and R. C. Barr, "The four-electrode resistivity technique as applied to cardiac muscle," *IEEE Transactions on Biomedical Engineering*, vol. 29, no. 7, pp. 541–546, 1982.

[10] P. Le Guyader, F. Trelles, and P. Savard, "Extracellular measurement of anisotropic bidomain myocardial conductivities. I. Theoretical analysis," *Annals of Biomedical Engineering*, vol. 29, pp. 862–877, 2001.

[11] P. Le Guyader, P. Savard, R. Guardo, L. Pouliot, F. Trelles, and M. Meunier, "Myocardial impedance measurements with a modified four electrode technique," *16th IEEE-EMBS*, pp. 880–881, 1994.

[12] R. C. Barr and R. Plonsey, "Electrode systems for measuring cardiac impedances using optical transmembrane potential sensors and interstitial electrodes — Theoretical design," *IEEE Transactions on Biomedical Engineering*, vol. 50, no. 8, pp. 925–934, 2003.

[13] D. D. Streeter, "Gross morrphology and fiber geometry of the heart," in *Handbook of Physiology, Vol 1*, R. M. Berne, Ed., chapter 2: The Cardiovascular System, pp. 61–112. Williams and Williams, Baltimore, MD, 1979.

[14] I. J. Legrice, P. J. Hunter, and B. H. Smail, "Laminar structure of the heart: a mathematical model," *American Journal of Physiology*, vol. 272, pp. H2466–H2476, 1997.

[15] Q. Li, *(in preparation)*, Ph.D. thesis, University of Tasmania, 2005.

[16] O. H. Schmitt, "Biological information processing using the concept of interpenetrating domains," in *Information Processing in the Nervous System*, K. N. Leibovic, Ed., chapter 18, pp. 325–331. Springer–Verlag, New York, 1969.

[17] L. Tung, *A Bi–domain model for describing ischaemic myocardial D-C potentials*, Ph.D. thesis, Massachusetts Institute of Technology, June 1978.

[18] W. T. Miller and D. B. Geselowitz, "Simulation studies of the electrocardiogram I: The normal heart," *Circulation Research*, vol. 43, pp. 301–315, 1978.

[19] P. Colli-Franzone and L. Guerri, "Spreading of excitation in 3–D models of the anisotropic cardiac tissue I: Validation of the eikonal model," *Mathematical Biosciences*, vol. 113, pp. 145–209, 1993.

[20] W. Krassowska and J.C. Neu, "Effective boundary conditions for syncytial tissues," *IEEE Transactions on Biomedial Engineering*, vol. 41, no. 2, pp. 143–150, 1994.

[21] William H. Press, Brian P. Flannery, Saul A. Teukolsky, and William T. Vetterling, *Numerical Recipes, The Art of Scientific Computing*, Cambridge University Press, Cambridge, 2nd edition, 1992.

[22] B. J. Roth, "Electrical conductivity values used with the bidomain model of cardiac tissue," *IEEE Transactions on Biomedical Engineering*, vol. 44, no. 4, pp. 326–328, April 1997.

[23] S. Weidmann, "Electrical constants of trabecular muscle from mammalian heart," *J. Physiol.*, vol. 210, pp. 1041–1054, 1970.